Preliminary Sky Mapping Trades

Lulu Liu

July 25th, 2007

Contents

1 Introduction

This document outlines a first analysis of detailed sky-mapping strategies for the TESS satellite mission with scientific considerations in mind. The mission looks to detect nearby transiting extrasolar planets with the objective of covering as much of the sky as possible in a short duration (two year) survey. A final sky-mapping plan would need to take into account a number of factors including the position of the sun (which would determine operations cycle of the satellite), interference from the moon (which would force the shut-off of affected cameras), and the number and character of our target stars and planets. We will look specifically at two similar but distinct configurations for two-year sky coverage and by comparing their merits and limits gain an understanding of the trades involved in the decision.

2 Mission Parameters

Several decisions have been made about the mission which provide us with the parameters we need to begin our analysis. Some decisions are final while others still stand to be revisited, however, we will assume these as our guides and adjust accordingly if they happen to change.

Equatorial Orbit A previous trade study set the satellite's orbit as equatorial - or no more than a few degrees inclined from the equator around the earth. This puts the constraint on our operations that we can only observe during what we call "orbit-night", when the satellite is in the earth's shadow during its 90 minute low-earth orbit.

Square Array We will have a 3×3 array of wide-angle cameras each with a non-overlapping field of view 18° by 18° wide. They are pointed so that each of three cameras in a column cover adjacent field in the sky but each of the three columns are separated by 18° in pointing direction. This setup allows for an easy 18° slew of the cameras halfway through each duty cycle to cover twice the amount of sky. The end result is that each orbit night, a block of sky 54° by 108° will be observed. See Figure 1.

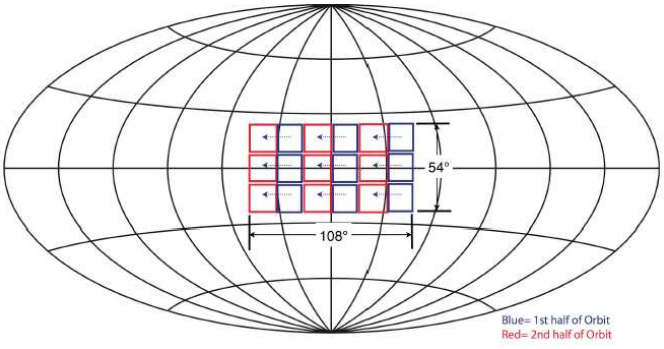

Figure 1: The 3×3 arrangement of cameras and the 18° slew mid-orbit.

Target Planets with Periods $<$ 60 Days Finding planets with orbits of at most 60 days requires 120 days of continuous observation for each part of the available sky. In order to achieve the photometric precision necessary to detect very small changes in light intensity, each star needs to map to the same pixels on the CCD orbit after orbit. In order to achieve this we use the stare-and-step method of observation– *stare* at only one part of the sky for 120 days and *step* to the next field and do the same.

Galactic Plane Noise Within approximately 10° of the Galactic Plane, the density of stars from our own Milky Way is too high to allow for reliable photometry as it creates crowding errors. Though it does not need to be avoided, the data collected from this part of the sky will be discarded.

Moon Avoidance Staring at a light source as intense as the moon may damage our instruments. We will need to shut off the cameras that will be affected by moonlight at any given time.

Two-Year Survey The mission will take place over approximately two years.

Nov. 1st, 2009 Mission Start Date For the purposes of this study, we will assume the proposed launch date of November 1st, 2009 to be the mission start date and 12:00 A.M. to be the mission start time.

3 Tools and Methods

I used STK (Satellite Tool Kit by AGI) and MATLAB (by Mathworks) to conduct this study.

In STK I modeled the scenario using the included ephemeris and orbital capabilities. Each camera was modeled as a sensor and fixed in direction with respect to the body of the satellite in accordance with the mission parameters. The attitude of the satellite itself was then adjusted to control the general pointing direction. The attitude was defined by two vectors, an aligning vector and a constraining vector. I chose the former based on where I wanted to point the center of the array of sensors (cameras), and the latter defined a rotation about the former. The Galactic Plane was defined with the Galactic North vector and used for visualization purposes.

Certain pointing constraints had to be imposed on each sensor (camera) to define non-observation times. For this model I used the sunlight requirement of umbra or penumbra and a minimum grazing angle (between line of sight and line tangent the earth) of 25°.

Data output from STK came in the form of reports. Reports can be generated about a whole range of parameters and values. The relevant reports were then processed in MATLAB using a series of custom scripts to yield meaningful graphs and summaries.

4 General Considerations

A field is defined as the entire $54° \times 108°$ area observed each orbit by the array of cameras. It is fixed in the sky. As a result of the 18° slew mid-orbit, each star in a field is surveyed for only half of orbit-night. This was a trade we were willing to make for twice the coverage.

Since each field as a whole needs to be observed continuously for 120 days, in two years we can observe exactly six distinct fields. As the geometry of these six fields will have a large impact on the mission operation, their arrangement, or configuration, is what I will explore here.

4.1 Field Accessibility

Each point in the sky (with exception of the Ecliptic North and South Poles) is optimal for observation only once a year– when it is most near anti-solar as seen from the earth. At this time it is centered in the earth's shadow, allowing for the longest duration unobstructed access in darkness. This optimal center shifts by approximately one degree per day ($360°/365 \text{ days} \approx 1°/\text{day}$), so we would expect the accessibility (defined as the

duration per orbit of unobstructed observation time) of any one field to drop off linearly on either side of its optimal peak. Access is calculated for the center point of each field.

Observation of any field would be most effective around its optimal access peak. Therefore we aim to build 120-day data-collecting phases around these peaks for each of the six fields. No field will be covered twice, no field can be omitted, and the telescope should be active and collecting meaningful data at all possible times. Figure 2 is a graphical representation of the above mentioned.

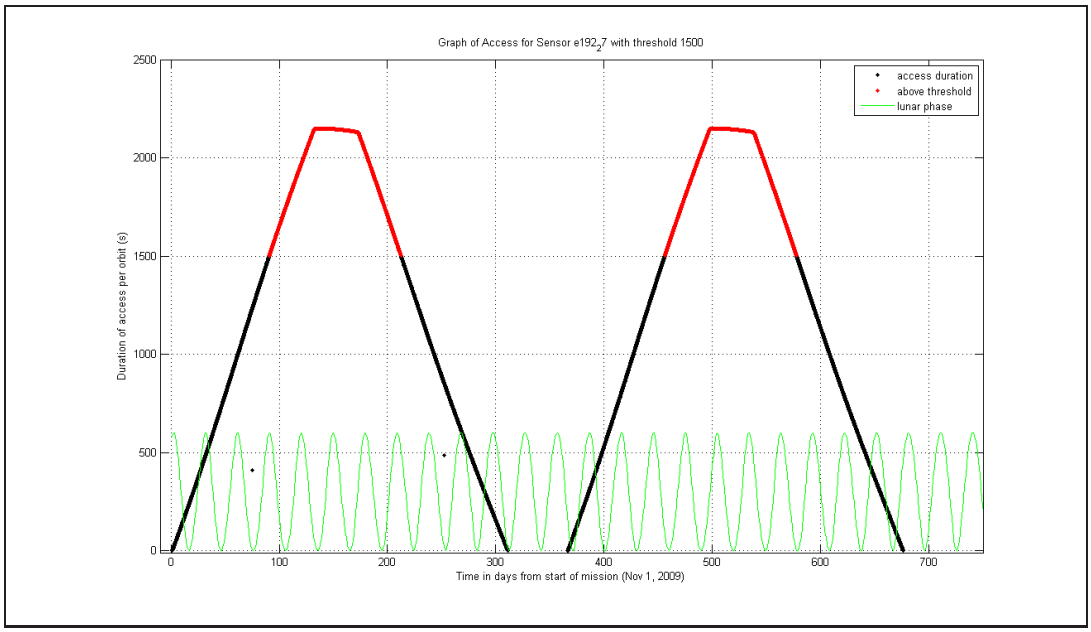

Figure 2: Access duration per orbit for the field centered around a point at RA 12° and Dec -27°. Notice the two peaks of optimal access over the period of two years and the highlighted regions of 120 days during which this field can be surveyed.

4.2 Field Uniformity

Any field in the sky with a non-zero area will be subject to accessibility variation from region to region. When we optimize for the center of the field, we are in essence taking an average over all the points in the field and observing when this representative is at its most accessible. As all regions of a field must be observed simultaneously, this will in fact ensure the most meaningful results from every region. Despite our efforts, variation across a field, especially at its edges, can be quite large, resulting in poor overall coverage of certain regions. On the other hand, several factors (including the equatorial orbit of the satellite and the more equatorial than polar path of the sun) come together to produce a much steeper error gradient in the horizontal than vertical direction. We can use this information to determine the most efficient orientation of each field.

4.3 Lunar Orbit

120 days is four times the period of the moon. Any cameras that point to a part of the lunar orbit will be interrupted (at least) four times during its data collection. There are

several ways to cope with this issue. First, we can "fill in" observation time at a later date by revisiting fields significantly affected by lunar interference. Though a useful maneuver, this solution is not a complete fix as some of our science will be compromised by the discontinuous nature of the data collection. Another thought is the avoidance of the lunar orbit altogether. This is clearly not possible for all the fields (as the lunar orbit is inclined at a significant angle with respect to the galactic plane) but perhaps our configuration could allow several fields to collect less fragmented or altogether uninterrupted data.

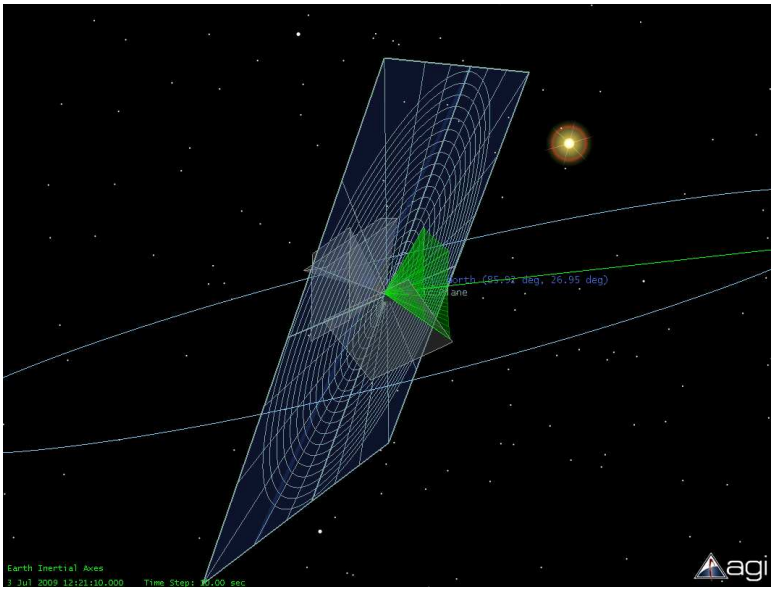

Figure 3: An STK visualization of the lunar orbit, the galactic plane, the sun, and several non-mission-specific sensors.

4.4 Total Integration Time

Total integration time can be a useful standard of comparison between different configurations. It is defined here as the total length of time during which a camera is collecting meaningful data. If Camera A were on for days 1-3, shut off, and reactivated for days 5-6, the total integration time for Camera A would be 5 days. Since integration time combines both access data and lunar interference data, if calculated correctly, it can be a useful figure of merit representative of certain mission strategies.

4.5 Spacecraft Attitude

Though a relatively minor concern when one is optimizing for science, it would be a mistake to omit spacecraft behavior and capabilities from our list of considerations. More complicated spacecraft maneuvers require more time to complete, excess power, and are more susceptible to errors and/or failure. Some strategies in spacecraft attitude adjustment have been proposed to better suit the science requirements, but in the end, more is dependent on a simple and considerate science plan.

5 Common Proposal

After some analysis I propose that efficient sky-mapping plans under the given parameters would, in addition to abiding by all the constraints of the mission, have the following in common:

1. *Vertical Mid-Orbit Slew.* Each field's long dimension (108° side) would be more or less lined up with longitudes on earth. This is accomplished by orienting the spacecraft so that the 18° slew halfway through each orbit-night is vertical instead of horizontal. There are two main motivations for this orientation. First, we achieve the highest field uniformity by aligning the shortest edge of the field against the steepest accessibility gradient, allowing us to optimize for all points in the field at the same time without too much loss. But just as importantly, since accessibility variation occurs mostly along the latitudes, six vertical fields can fit around the celestial sphere without much (or any) horizontal overlap, and therefore without much overlap in optimal observation times. This ensures that each field can be observed at a different time in the mission and none will be missed.
2. *∼120° Spacing Between Fields.* The location of a field is defined by the point at its center. The center of each field should be 120° in RA from the center of another if they are to be observed back-to-back. This is again a direct effect of the 1° per day shift of the earth umbra cone. During the 120 day observation of any field, the optimal region would have shifted by 120° in the sky, landing it right on top of the next active field.
3. *Symmetry Across the Galactic Plane.* There should not be a preference for either side of the Galactic Plane. In addition, no field should span the galactic plane, as much of what it observes will then be meaningless.
4. *Free Observation Time.* Whether at the beginning, the middle, or the end of the survey, it is important to set aside a block of obligation-free time to take care of issues that might arise. At best, this window of time would be useful for "filling in" gaps in the survey caused by the presence of the moon. At worst, it would provide for schedule flexibility in case of unexpected interruptions.

6 A Detailed Study of Two Configurations

Keeping in mind the previously discussed constraints and considerations, I modeled two separate sky-mapping strategies and conducted a detailed analysis of each. The strategies themselves are distinct only in that they cover somewhat different regions of the sky– that is, their assigned fields have different centers and small disparities in alignment. My analysis yields an observation schedule, access graphs and data, lunar interference patterns and intervals, and total integration statistics per camera, per field, and per configuration.

6.1 Configuration One

The focus of this particular set-up is total avoidance of the galactic plane and partial avoidance of the moon. These are achieved through the sacrifice of at most 5-10% of sky coverage due to overlapping fields.

6.1.1 Layout

The six target fields in the sky are distributed evenly on either side of the galactic plane. The three fields on one side of the galactic plane are pictured in Figure 4. The other three

are determined by a rotation of 180° in any direction, creating antipodal associates for each of the first three sensors. Table 1 shows the location of each field in Configuration 1 marked by their centers. Each field's vertical dimension is constrained to be aligned with the longitudes of the earth.

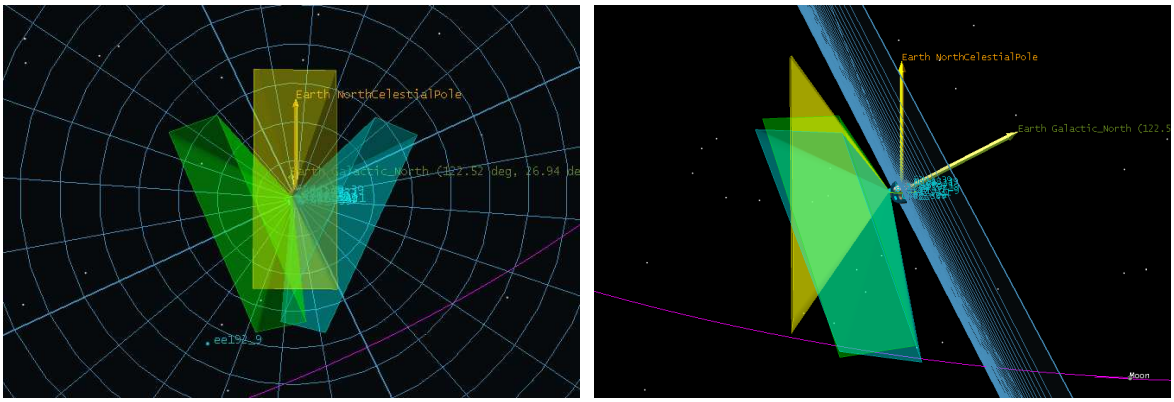

(a) Face-on view of Config 1

(b) Side view of Config 1

Figure 4: Three fields of Config 1 seen from the front and the side. These three fields are on the same side of the galactic plane. Green - A, Yellow - B, Blue - C. Other three fields not pictured.

Field	Right Ascension (°)	Declination (°)
A	-42	-30
B	12	0
C	66	-30
D	138	30
E	192	0
F	246	30

Table 1: Location of the six fields of Config 1.

6.1.2 Per Field Access

Access graphs like the example given in Section 4.1 are then computed for each field using a combination of STK and MATLAB for the duration of the two-year survey. Upon studying these graphs, it becomes evident that by conducting observations only when a field is above the accessibility threshold of 1500 seconds per orbit, we carve out survey segments of exactly 120 days for each field around its optimal peak. The six access graphs are reproduced in Figure 5 in spatial order.

The graphs in Figure 5 show that fields A, C, and E can be observed consecutively, since as one field dips below threshold the next comes immediately into range. Similarly, fields B, D, and F can be observed consecutively. This is logical to us since every other field is spaced approximately 120° apart. However, to switch between these two groups and generate the entire set of six fields, we must await a phase shift of approximately 60 days. This will be necessary halfway through the survey. These 60 days can be considered free observation time. With this in mind we create a mission observation schedule.

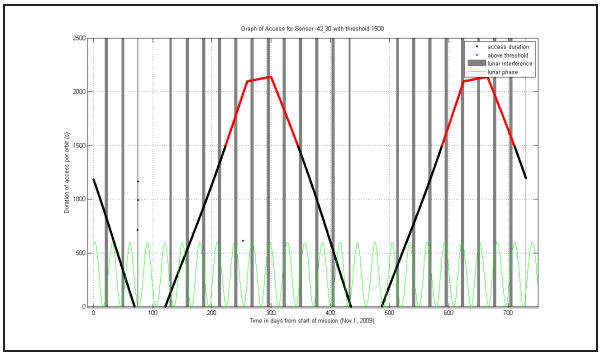

(a) RA: -42 Dec: -30

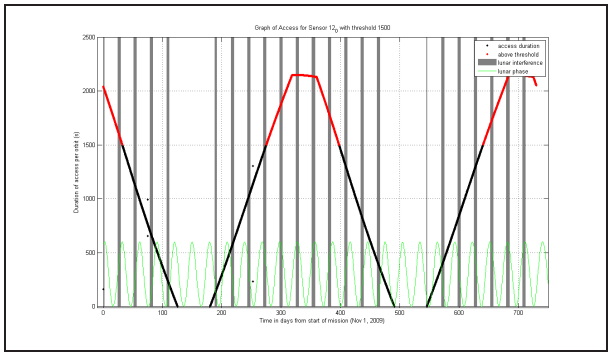

(b) RA: 12 Dec: 0

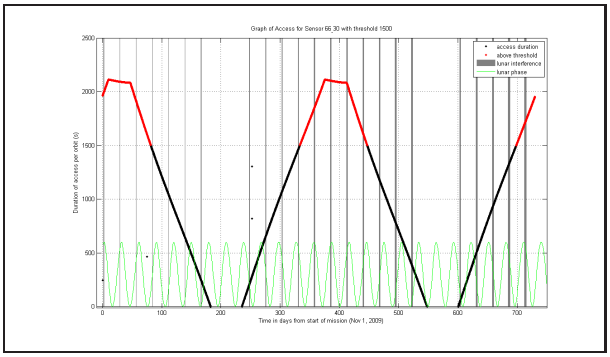

(c) RA: 66 Dec: -30

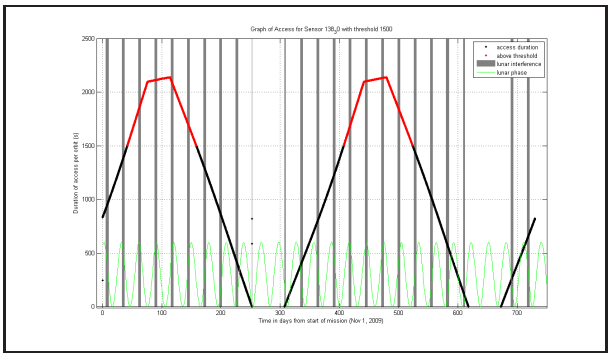

(d) RA: 138 Dec: 30

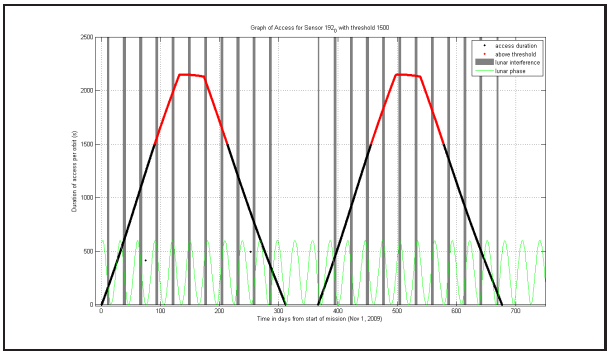

(e) RA: 192 Dec: 0

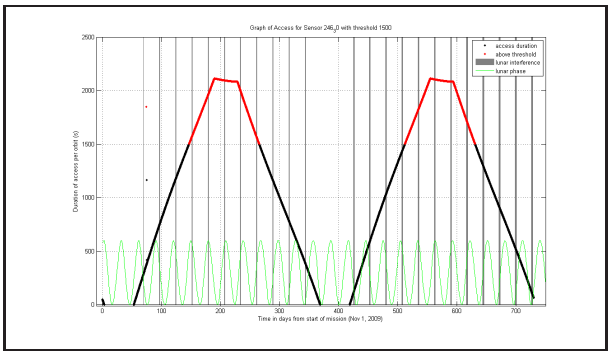

(f) RA: 246 Dec: 30

Figure 5: Per orbit access (s) vs. days since start of mission for all six fields in Config 1. The additional vertical grey bars represent approximate periods of lunar interference for each field.

6.1.3 Observation Schedule

Days Since Mission Start	Active Field Name	Active Field Description
0-40	–	In-Orbit Check-Up and Maintenance
40-160	D	RA: 138 Dec: 30
160-280	F	RA: 246 Dec: 30
280-400	B	RA: 12 Dec: 0
400-460	–	Free Observation Time
460-580	E	RA: 192 Dec: 0
580-700	A	RA: -42 Dec: -30
700-820	C	RA: 66 Dec: -30

6.1.4 Per Camera Access and Lunar Data

Restricting each field to its active interval, we can break down the single sensor representing a field into its individual subfield components. We treat the "bottom" and "top" halves of each field independently to gather data about the cameras before and after the 18° mid-orbit slew. The naming scheme for each subfield is simple: for example, in field A, the bottom half retains the name A, while the top half is relabeled field AA, and the number following each field designation indicates the camera responsible for its observation. Figure 6 shows the array of subfields and their associated names for all of the original field A while Figure 7 shows the array of 9 cameras (modeled as sensors) as seen in STK.

AA-1	*AA-2*	*AA-3*
A-1	A-2	A-3
AA-4	*AA-5*	*AA-6*
A-4	A-5	A-6
AA-7	*AA-8*	*AA-9*
A-7	A-8	A-9

Figure 6: Array of cameras 1-9 pointing at field A. The A subfields and AA subfields will each be observed for one half of the duty cycle.

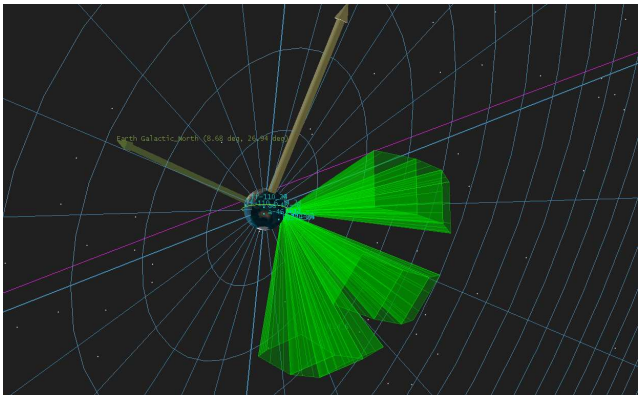

Figure 7: Model of the array of 9 sensors in STK.

We use STK to generate the following reports for each field during its active time period: *access intervals per camera* (includes statistics about total integration time for each camera) and *the location of the moon with respect to each camera* (measured in angle in degrees between boresight vector of each sensor and vector to the moon). A total of 12 sets of data are generated– two (top and bottom) for each field. The access reports for each camera and each field are kept for later integration time computations. Meanwhile, we will focus on the lunar interference statistics– possibly the most important set of data to come out of the analysis.

First, a threshold needs to be set for the minimum observing angle to the moon ($\theta_{min}(t)$). If the moon comes within this angle the affected camera(s) will be turned off. This threshold is not a constant. It is intuitive that the brighter (fuller) the moon, the larger this value would need to be to account for scattered light. Without full instrument specifications, we can only use a general function to approximate this variation. This simple function assumes a linear relationship between the light scattering effects and the percent fullness of the moon ($\phi(t) \in [0,100]$). It uses a minimum value of 20 degrees for a new moon (0% full), a maximum value of 30 degrees for the full moon, and is reproduced below.

$$\theta_{min}(t) = 20 + 0.1\phi(t) \tag{1}$$

More generally, the equation would be (with m for min and M for max):

$$\theta_{min}(t) = m + \frac{M-m}{100}\phi(t) \tag{2}$$

Since lunar phase ($\phi(t)$) is a sinuisoid, it follows that this function is also sinusoidal in character. Data for "fields" A and AA are plotted in Figure 8 along with the threshold curve. The lunar phase is there for reference.

Numerically, the intervals are collected in a text file. Not only will this data be useful for the current analysis, they will also serve as input for future window function calculations as well as provide the camera shut off times for the on-board telescope. The examples for cameras 1 and 9 during observation of field A follow. It's important to keep in mind that these are unconstrained values. They are taken assuming constant pointing for continuous plots. They are defined by a fixed boresight vector in space (within the 120 days) and a rotating lunar location vector. You will see this subtlety come into play when calculating total integration time.

Table 2: Lunar Interference Intervals for Camera 1 of Field A

Start Time	Start Angle	Start Lunar Phase	End Time	End Angle	End Lunar Phase
592.25	29.92	99.00	596.24	28.52	87.00
619.54	29.22	95.00	623.66	29.70	96.00
647.04	27.93	79.00	650.96	29.99	100.00
674.36	25.90	55.00	678.22	29.11	90.00

Table 3: Lunar Interference Intervals for Camera 9 of Field A

Start Time	Start Angle	Start Lunar Phase	End Time	End Angle	End Lunar Phase
none					

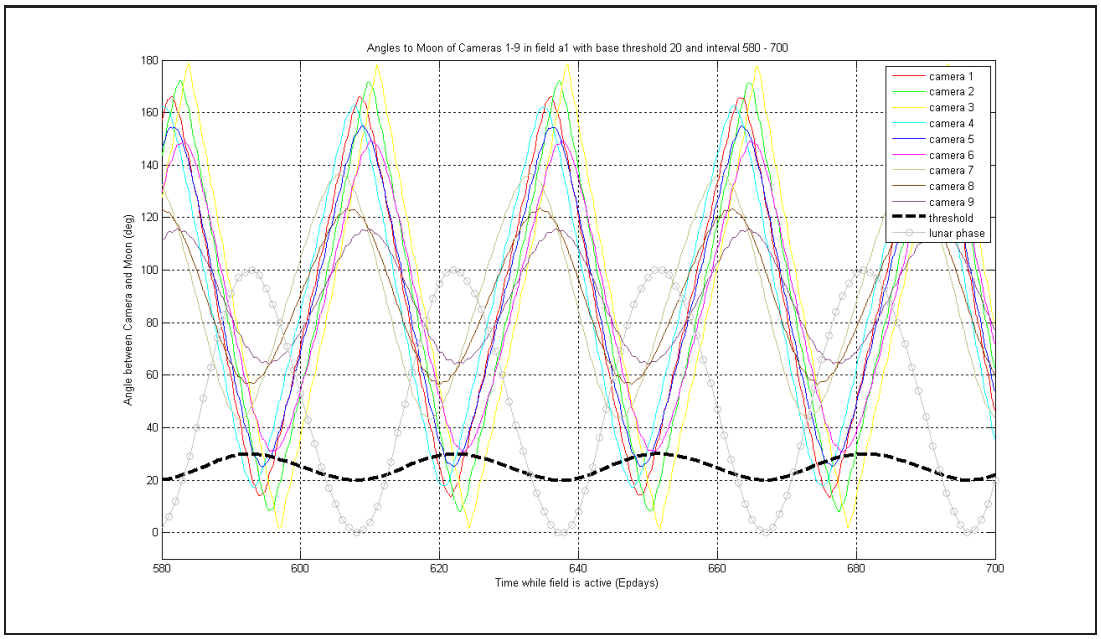

(a) field A

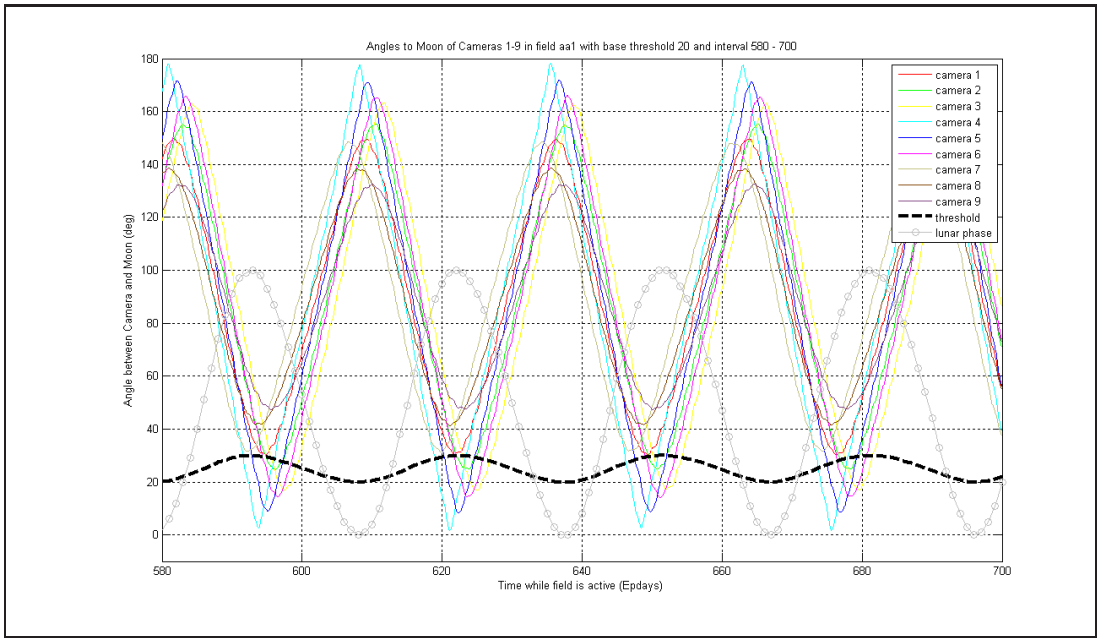

(b) field AA

Figure 8: Each camera's line-of-sight angle to the moon as a function of days since start of mission.

Of course, this analysis for a few fields is extensible to the rest of the configuration with the appropriate intervals in mind. Finally, we will condense this data into a few simple figures and values with total integration time.

6.1.5 Total Integration Statistics

Again, total integration time is used to describe the total duration of useful data collection. The two largest contributors to variations in total integration time are the uniformity of the field (how far off-peak we are observing) and the periodic interference from the moon. An approximate total integration time for each camera subfield (τ_c) is computed in the following manner:

1. Generate a lunar interference fraction using the ratio between total interference time (sum of the lengths of all interference intervals α_i) and the entire observation period of 120 days.
2. Multiply this fraction by the total access time (T) from the camera to the subfield in days (a conversion may be necessary).
3. Since any subfield is observed for only one half of each orbit-night, we multiply the result by $\frac{1}{2}$.

In equation form,

$$\tau_c = \frac{T}{2} \cdot \frac{1}{120} \left(\sum \alpha_i \right), \tag{3}$$

where the summation is taken over all intervals α_i.

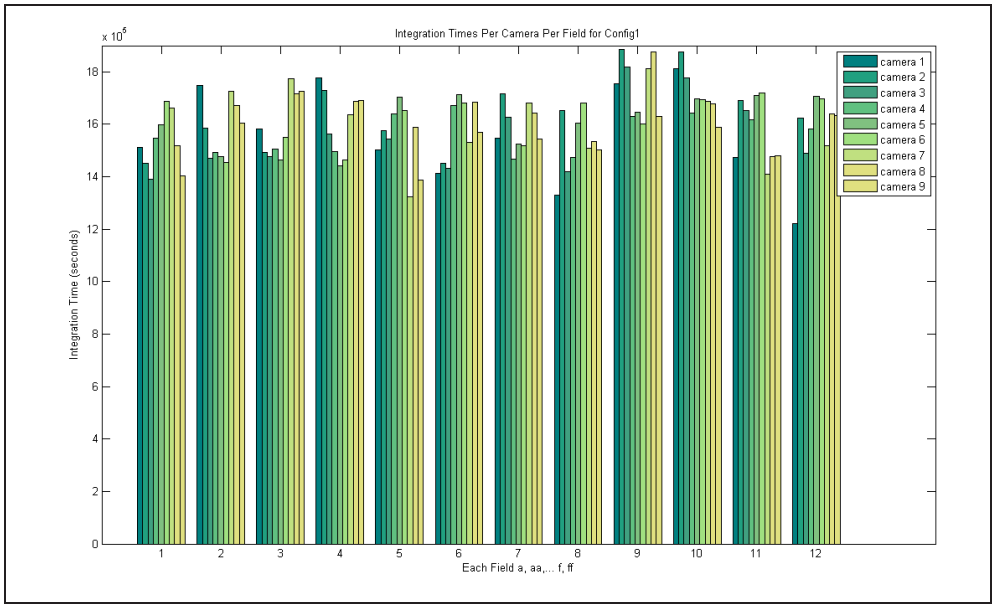

Figure 9: Total integration time per camera subfield. Grouped by field (A, AA, B, BB... F, FF).

Notice in Figure 9 that field E and EE have a significantly higher average per subfield integration time. This is a result of the slight lunar avoidance of this particular configuration. Further lunar avoidance can always be explored.

We take the average integration time over all the cameras of a field and consider that the total integration time for the field,

$$\tau_f = \bar{\tau_c} = \frac{1}{9} \cdot \sum_{j=1}^{9} \tau_{cj} \tag{4}$$

Sum over all fields in this configuration for the final value of τ_I for Configuration 1.

$$\boxed{\tau_I \approx 19,141,148 \; sec \approx 221.5 \; days}$$

This ends the analysis for the first configuration of sensors. Next we choose different fields in the sky.

6.2 Configuration Two

Configuration two optimizes for sky coverage. In this case we aim for little to no overlapping of fields. As a result, a full 35,000 square degrees is observed, approximately 2000-3000 square degrees greater than what is surveyed in the first pointing plan. However, there can be no lunar avoidance and the edges of some fields come well within 10° of the Galactic Plane. The loss here will be about 10%.

Since this analysis is a repeat of the first, only data will be presented. For the procedure, please see Configuration 1, section 6.1.

6.2.1 Layout

Once more, the six target fields are distributed evenly on either side of the Galactic Plane. The fields again are defined by their centers. This time, each field's vertical dimension is constrained against a projection of the earth celestial north vector onto the Galactic Plane (labeled as Earth Vector1 in the figure). See Figure 10.

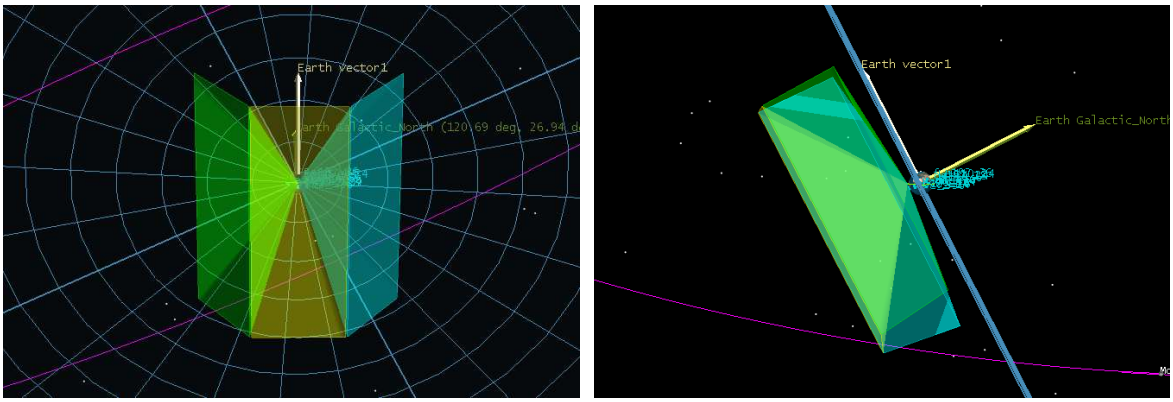

(a) Face-on view of Config 2

(b) Side view of Config 2

Figure 10: Three fields of Config 2 seen from the front and the side. These three fields are on the same side of the galactic plane. Green - A, Yellow - B, Blue - C. Other three fields not pictured.

Field	Right Ascension (°)	Declination (°)
A	-46	-15
B	12	-27
C	70	-15
D	134	15
E	192	27
F	250	15

Table 4: Location of the six fields of Config 2.

6.2.2 Observation Schedule

The per field access for Configuration 2 is nearly identical to that of Configuration 1. Naturally, the observation schedule looks familiar.

Days Since Mission Start	**Active Field Name**	**Active Field Description**
0-40	–	In-Orbit Check-Up and Maintenance
40-160	D	RA: 134 Dec: 15
160-280	F	RA: 250 Dec: 15
280-400	B	RA: 12 Dec: -27
400-460	–	Free Observation Time
460-580	E	RA: 192 Dec: 27
580-700	A	RA: -46 Dec: -15
700-820	C	RA: 70 Dec: -15

6.2.3 Results of the Analysis

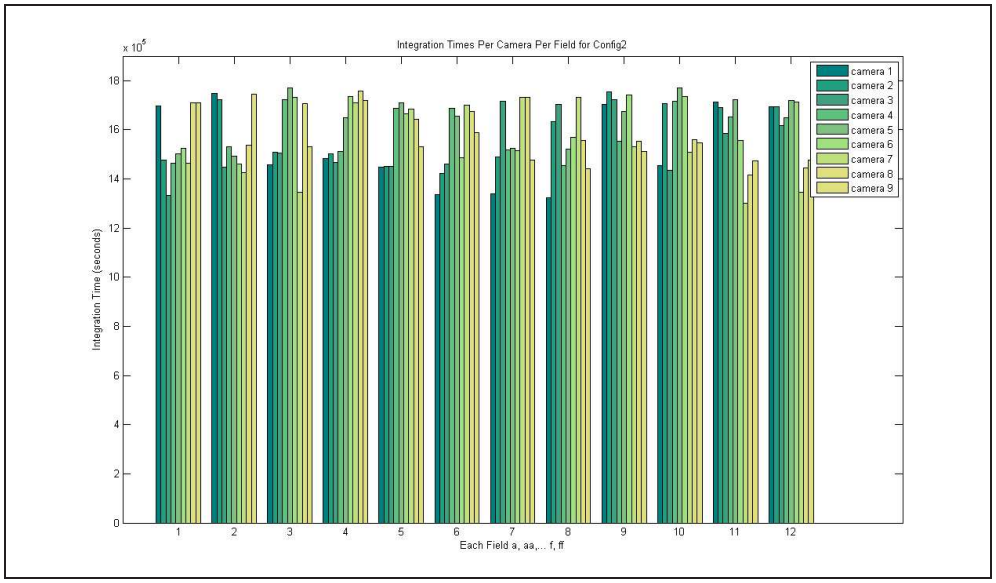

Figure 11: Configuration 2 total integration time per camera subfield. Grouped by field (A, AA, B, BB... F, FF).

And the τ_{II} final value for Configuration 2:

$$\boxed{\tau_{II} \approx 18,970,360 \; sec \approx 219.5 \; days}$$

7 Conclusions

Although the two configurations are essentially as different as allowable under the mission parameters and the guidelines set by the common proposal, over the period of two years, the disparity between them in terms of total observation time is only about two days. This is a promising result that tells us of the stability of this general pointing strategy. Since Configuration 1 shows the fields at their most staggered (vertically divergent) and Configuration 2 at their least (aligned), we can be assured that under the guidelines drawn no configuration will yield drastically dissimilar results. Though we do not in fact have a clear cut answer for the nebulous question of "best", we now have flexibility to pursue whatever goals may become important to us in the future. For example, when the analysis is completed for the expected yield of stars, we can assign the fields to cover regions with the most promising star profiles. In addition, our partners at the Harvard-Smithsonian Center for Astrophysics are devising a list of tens of thousands of bright target stars. Flexibility in pointing strategy is welcomed, as we hope to be able to accommodate as many of those stars into our search as possible.